

Synthesis and Characterization of $[\text{Mn}^{\text{III}}_6(\text{N-formylsalicylhydrazidate})_6(\text{MeOH})_6]$: A New Type of Macrocyclic Hexanuclear Manganese Cluster

Byunghoon Kwak,[†] Hakjune Rhee,[†] Soonheum Park,[‡] and Myoung Soo Lah*[†]

Department of Chemistry, College of Science, Hanyang University, 1271 Sa-1-dong, Ansan, Kyunggi-do 425-791, Korea, and Department of Chemistry, College of Natural Science, Dongguk University, Kyung-Ju 780-714, Korea

Received December 9, 1997

The macrocyclic hexanuclear metal cluster, $[\text{Mn}^{\text{III}}_6(\text{fshz})_6\text{S}_6]$, **1** (S = MeOH), was prepared using a trianionic pentadentate ligand, *N*-formylsalicylhydrazidate (fshz^{3-}). Due to the meridional coordination of the ligand to the metal ion, the ligand is not only bridging the ring metal ions using a hydrazide N–N group but also enforcing the stereochemistry of the metal ions as a propeller configuration. The alternations of the chiralities of the metal centers expand the cyclic ring system of complex **1** to the 24-membered ring system. The neutral hexanuclear manganese complex with noncrystallographic pseudo- C_{3i} symmetry is in the crystallographic inversion center. The disc-shaped hexanuclear cluster is 1.8 nm in diameter and 0.8 nm in thickness and has a vacant cavity in the center of the cluster. Three solvent molecules coordinated at the metal centers with Λ configuration are in one face of the cluster, and the remaining three solvent molecules coordinated at the other metal centers with Δ configuration are in the other face of the cluster. The two faces of the cluster have opposite chiralities to each other. The crystal packing structure of complex **1** shows that the disc-shaped hexanuclear clusters are aligned approximately along the crystallographic *a* axis. The cavities of the clusters in the crystal structure are also aligned, and one-dimensional channels are formed. The solution integrity of the cluster was addressed using solution mass spectrometry, paramagnetically shifted ^1H NMR spectroscopy, and UV–visible spectroscopy. Crystallographic data for **1**: triclinic, $P\bar{1}$, $a = 10.0237(9)$ Å, $b = 15.096(1)$ Å, $c = 15.617(1)$ Å, $\alpha = 112.142(5)^\circ$, $\beta = 106.615(5)^\circ$, $\gamma = 99.958(7)^\circ$, $V = 1989.8(3)$ Å³, $Z = 2$, $D_{\text{calcd}} = 1.510$ g cm⁻³, $R1 = 0.0502$ and $wR2 = 0.1424$ for 4249 reflections with $I > 2\sigma(I)$, GOF = 1.065.

Introduction

Supramolecular chemistry, self-assembly, host–guest chemistry, and molecular recognition are at the forefront of modern chemistry.¹ Most of the studies are focused on organic host molecules, while inorganic host molecules receive much less attention. Recently self-assembled metal clusters, macrocyclic squares,² mercuracarborand cyclic species,³ and metal analogues of calix[4]arene⁴ have appeared as new types of the inorganic host molecules.

Another type of metal cluster, known as a metallacrown,^{5,6} has also emerged as inorganic host molecules. The metallacrowns could be synthesized using multidentate ligand that could bridge two metal ions as shown in Figure 1A. The cyclic repetition of the ligand bridging of two metal ions generates the macrocyclic metal cluster. Metallacrowns can recognize

cations with the donor atoms of the central cavity and bridging ligands and can also recognize anions using the ring metal ions and the captured cation.^{5d} Nine-membered,^{5a–c} twelve-membered,^{5a,d–j} and fifteen-membered metallacrowns^{5k,l} have been developed up to date.

In this study, we synthesized a new potential pentadentate ligand, *N*-formylsalicylhydrazide (H_3fshz). The triply deprotonated *N*-formylsalicylhydrazidate (fshz^{3-}) may bridge the metal ions using a hydrazide N–N group as shown in Figure 1B. In addition, the meridional coordination of the fshz^{3-} to the metal ion may force the neighboring ligands into only the propeller configuration.

[†] Hanyang University.

[‡] Dongguk University.

- (1) (a) Grotzfeld, R. M.; Branda, N.; Rebek, J., Jr. *Science* **1996**, *271*, 487–489. (b) Asakawa, M.; Ashton, P. R.; Ballardini, R.; Balzani, V.; Belohradsky, M.; Gandolfi, M. T.; Kocian, O.; Prodi, L.; Raymo, F. M.; Stoddart, J. F.; Venturi, M. *J. Am. Chem. Soc.* **1997**, *119*, 302–310.
- (2) (a) Olenyuk, B.; Whiteford, J. A.; Stang, P. J. *J. Am. Chem. Soc.* **1996**, *118*, 8221–8230. (b) Slone, R. V.; Hupp, J. T.; Stern, C. L.; Albrecht-Schmitt, T. E. *Inorg. Chem.* **1996**, *35*, 4096–4097. (c) Fujita, M.; Sasaki, O.; Mitsuhashi, T.; Fujita, T.; Yazaki, J.; Yamaguchi, K.; Ogura, K. *J. Chem. Soc., Chem. Commun.* **1996**, 1535–1536.
- (3) Zheng, Z.; Knobler, C. B.; Mortimer, M. D.; Kong, G.; Hawthorne, M. F. *Inorg. Chem.* **1996**, *35*, 1235–1243.
- (4) Rauter, H.; Hillgeris, E. C.; Erxleben, A.; Lippert, B. *J. Am. Chem. Soc.* **1994**, *116*, 616–624.

- (5) (a) Lah, M. S.; Pecoraro, V. L. *Comments Inorg. Chem.* **1990**, *11*, 59. (b) Gibney, B. R.; Stemmler, A. J.; Pilotek, S.; Kampf, J. W.; Pecoraro, V. L. *Inorg. Chem.* **1993**, *32*, 6008–6015. (c) Lah, M. S.; Kirk, M. L.; Hatfield, W.; Pecoraro, V. L. *J. Chem. Soc., Chem. Commun.* **1989**, 1606–1608. (d) Gibney, B. R.; Wang, H.; Kampf, J. W.; Pecoraro, V. L. *Inorg. Chem.* **1996**, *35*, 6184–6193. (e) Gibney, B. R.; Kampf, J. W.; Kessissiglou, D. P.; Pecoraro, V. L. *Inorg. Chem.* **1994**, *33*, 4840–4849. (f) Lah, M. S.; Pecoraro, V. L. *Inorg. Chem.* **1991**, *30*, 878–880. (g) Lah, M. S.; Pecoraro, V. L. *J. Am. Chem. Soc.* **1989**, *111*, 7258. (h) Kurzak, B.; Farkas, E.; Glowiak, T.; Kozłowski, H. *J. Chem. Soc., Dalton Trans.* **1991**, 163–167. (i) Stemmler, A. J.; Kampf, J. W.; Pecoraro, V. L. *Inorg. Chem.* **1995**, *34*, 2771–2772. (j) Lah, M. S.; Gibney, B. R.; Tierney, D. L.; Penner-Hahn, J. E.; Pecoraro, V. L. *J. Am. Chem. Soc.* **1993**, *115*, 5857–5858. (k) Stemmler, A. J.; Barwinski, A.; Baldwin, M. J.; Victor Y.; Pecoraro, V. L. *J. Am. Chem. Soc.* **1996**, *118*, 11962–11963. (l) Kessissiglou, D. P.; Kampf, J. W.; Pecoraro, V. L. *Polyhedron* **1994**, *13*, 1379–1391.
- (6) (a) Blake, A. J.; Gould, R. O.; Grant, C. M.; Milne, P. E.; Reed, D.; Winpenny, E. P. *Angew. Chem., Int. Ed. Engl.* **1994**, *33*, 5–197. (b) Blake, A. J.; Gould, R. O.; Milne, P. E.; Winpenny, E. P. *J. Chem. Soc., Chem. Commun.* **1991**, 1453–1454.

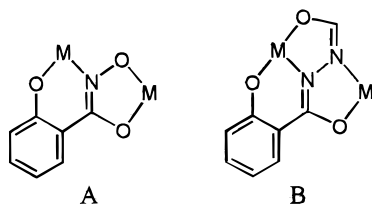


Figure 1. (A) Binding sites of shi^{3-} : Six- and five-membered chelating rings. (B) Binding sites of fshz^{3-} : Six-, five-, and five-membered chelating rings.

Experimental Section

Materials. The following were used as received with no further purification: salicylhydrazide, trimethylacetyl chloride, formic acid, triethylamine, and acetone- d_6 from Aldrich, Inc.; manganese acetate tetrahydrate from Yakuri; acetone, diethyl ether, chloroform, hexane, methanol (MeOH), ethanol (EtOH), dimethylformamide (DMF), and tetrahydrofuran (THF) from Carlo Erba.

Characterization. C, H, N, and Mn determinations were performed by the Elemental Analysis Laboratory of the Korean Institute of Basic Science. Infrared spectra were recorded as KBr pellets in the range 4000–600 cm^{-1} on a Bio-Rad FT-IR spectrometer. Absorption spectra were obtained using Perkin-Elmer Lambda spectrometer. NMR spectra were obtained using a Varian-300 spectrometer. Positive-ion FAB mass spectra were obtained using a JEOL HX110A/HX110A tandem mass spectrometer in a 3-nitrobenzyl alcohol matrix. Room-temperature magnetic susceptibilities of well-ground solid samples were measured using an Evans balance. The measurements were calibrated against a $\text{Hg}[\text{Co}(\text{SCN})_4]$ standard.

Synthesis of the Ligand. A 4.12 mL (33.4 mmol) amount of trimethylacetyl chloride was added to a solution of 1.31 mL (33.4 mmol) of formic acid and 4.66 mL (33.4 mmol) of triethylamine in 60 mL of chloroform at 0 °C. The reaction mixture was then slowly warmed to 25 °C. When 4.238 g (27.9 mmol) of salicylhydrazide was added to the reaction mixture, a white suspension was obtained. The resulting suspension was filtered and rinsed with chloroform and diethyl ether (4.568 g, 91% yield). Mp: 171–172°. IR (KBr pellet): 3300, 3260, 3070, 1680, 1650, 1490, 1230, 750 cm^{-1} . ^1H NMR (300 MHz, $\text{DMSO}-d_6$): δ 11.83, 10.65, 10.40 (br s, br s, s, 3H, Hs at amides and phenolic OH), 8.16 (s, 1H, H at formyl), 7.90 (dd, 1H, $J = 7.9, 1.6$ Hz, H at phenyl), 7.45 (td, 1H, $J = 7.8, 1.5$ Hz, H at phenyl), 7.00–6.92 (m, 2H, Hs at phenyl). ^{13}C NMR (75.5 MHz, $\text{DMSO}-d_6$): δ 166.68, 159.57, 158.92, 134.47, 128.92, 119.48, 117.65, 114.99. Anal. Calcd for $\text{C}_8\text{H}_8\text{N}_2\text{O}_3$: C, 53.33; H, 4.48; N, 15.55. Found: C, 53.24; H, 4.44; N, 15.28.

Synthesis of the Manganese Complex. A 0.546 g (3.0 mmol) amount of H_3fshz was dissolved in 60 mL of methanol, and 0.735 g (3.0 mmol) of manganese(II) acetate tetrahydrate was dissolved in 60 mL of methanol in another flask. The two solutions were mixed and stirred. After 5 min of stirring the solution was filtered. After the solution stood for 4 days, it produced dark brown rectangular crystals (0.668 g, 84.4% yield). Anal. Calcd for $\text{Mn}_6(\text{fshz})_6(\text{H}_2\text{O})_6$ ($\text{Mn}_6\text{C}_{48}\text{H}_{42}\text{N}_{12}\text{O}_{24}$): C, 38.42; H, 2.82; N, 11.20; Mn, 21.97. Found: C, 38.69; H, 2.82; N, 11.45; Mn, 21.1. ^1H NMR (acetone- d_6): δ -10.1 (H3 at phenyl), -21.6 (H5 at phenyl), -34.9 (H4 at phenyl), 3.20 (Hs at H_2O). FAB mass spectrum: m/z of $[\text{Mn}_6(\text{fshz})_6 + \text{H}]^+$, 1393.5. UV-vis (THF) [λ_{max} (ϵ): 242 (168 000 $\text{M}^{-1} \text{cm}^{-1}$), 276 (131 000 $\text{M}^{-1} \text{cm}^{-1}$), 369 (19 600 $\text{M}^{-1} \text{cm}^{-1}$), 453 nm (4400 $\text{M}^{-1} \text{cm}^{-1}$). μ_{eff} : 11.73 μ_{B} (4.79 μ_{B} /metal).

X-ray Crystallography. Because crystal **1** loses its solvents of crystallization within 1 min, it was mounted in a glass capillary with the mother liquor to prevent the loss of the structural solvents during data collection. Preliminary examination and data collection for the crystal **1** were performed with Mo $\text{K}\alpha$ radiation ($\lambda = 0.71069$ Å) on an Enraf-Nonius CAD4 computer-controlled κ -axis diffractometer equipped with a graphite crystal, incident-beam monochromator. Cell constants and orientation matrix for data collection were obtained from least-squares refinement, using the setting angles of 25 reflections. Data were collected at room temperature using the ω scan technique. Three

Table 1. Crystal Data and Structure Refinement for **1**

formula	$\text{C}_{30.5}\text{H}_{41}\text{Mn}_3\text{N}_6\text{O}_{15.5}$
fw	904.51
temp	293(2) K
cryst system, space group	triclinic, $P\bar{1}$
unit cell dimens	$a = 10.0237(9)$ Å, $\alpha = 112.142(5)^\circ$ $b = 15.096(1)$ Å, $\beta = 106.615(6)^\circ$ $c = 15.617(1)$ Å, $\gamma = 99.958(7)^\circ$
V	1989.8(3) Å ³
Z , calcd density	2, 1.510 mg/m^3
abs coeff	1.011 mm^{-1}
cryst size	0.80 × 0.45 × 0.40 mm
θ range for data collcn	1.53–22.46°
reflens collcd/unique	5190/5189 [$R(\text{int}) = 0.0049$]
data/restraints/params	5189/4/514
goodness-of-fit on F^2	1.065
final R indices [$I > 2\sigma(I)$] ^a	$R1 = 0.0502$, $wR2 = 0.1424$
R indices (all data) ^a	$R1 = 0.0618$, $wR2 = 0.1497$
largest diff peak and hole	0.393 and $-0.328 \text{ e} \cdot \text{Å}^{-3}$

$$^a R1 = \sum ||F_o| - |F_c|| / \sum |F_o|. wR2 = [\sum w(F_o^2 - F_c^2)^2 / \sum wF_o^4]^{1/2}.$$

standard reflections were monitored every 1 h, but no intensity variations were monitored. Lorentz and polarization corrections were applied to the data; however, no corrections were made for absorption. The structure was solved by direct methods using SHELXS-86⁷ and refined by full-matrix least-squares calculations with SHELX-97.⁸ Several noncoordinating methanol sites were identified, and one of them was half-occupied. The C–O bond lengths of the noncoordinating methanols ranged from 1.04(4) to 1.46(2) Å. In the final stage of the refinement, the C–O bond lengths were restrained as an average C–O bond length of the coordinated methanols, 1.42 Å. All non-hydrogen atoms were refined anisotropically; hydrogen atoms were allowed to ride on geometrically ideal positions with isotropic temperature factors 1.2 times those of the attached non-hydrogen atoms. Crystal and intensity data are given in Table 1.

Results and Discussion

Macrocyclic hexanuclear metal cluster $[\text{Mn}^{\text{III}}_6(\text{fshz})_6(\text{MeOH})_6]$, **1**, was prepared using the trianionic pentadentate ligand fshz^{3-} . An ORTEP diagram of complex **1** is shown in Figure 2. Metrical parameters are found in Table 2. The pentadentate ligand is not only bridging the ring metal ions using a hydrazide N–N group but also forcing the stereochemistry of the metal ions into a propeller configuration due to the meridional coordination of the O1,⁹ N1, and O3 atoms of the ligand to the metal ion. All ring metal ions demonstrate the propeller configurations despite the Jahn–Teller distortion of high-spin d^4 manganese(III) ions. The typical Jahn–Teller elongation along the z -axis of the manganese(III) ion is observed. The average axial bond distance (the average value of Mn–O4 and Mn–N2 bond distances: 2.240 Å) is about 0.32 Å longer than the average basal bond distance (the average value of Mn–O1, Mn–O2, Mn–O3, and Mn–N1 bond distances: 1.923 Å). The neutral hexanuclear manganese complex with noncrystallographic pseudo- C_{3i} symmetry is in the crystallographic inversion center. Complex **1** is 1.8 nm in diameter and 0.8 nm in thickness. Complex **1** has a vacant cavity in the center of the cluster. The approximate dimensions of the oval-shaped cavity are about 2.7 Å in diameter at the entrance, about 6.9 Å at its largest diameter at the center of the cavity, and about 4.3 Å

(7) Sheldrick, G. M. *Acta Crystallogr.* **1990**, *A46*, 467.

(8) Sheldrick, G. M. *SHELX-97*; University of Göttingen: Göttingen, Germany, 1997.

(9) The labels of the atoms were presented without alphabetic characters, A, B, or C.

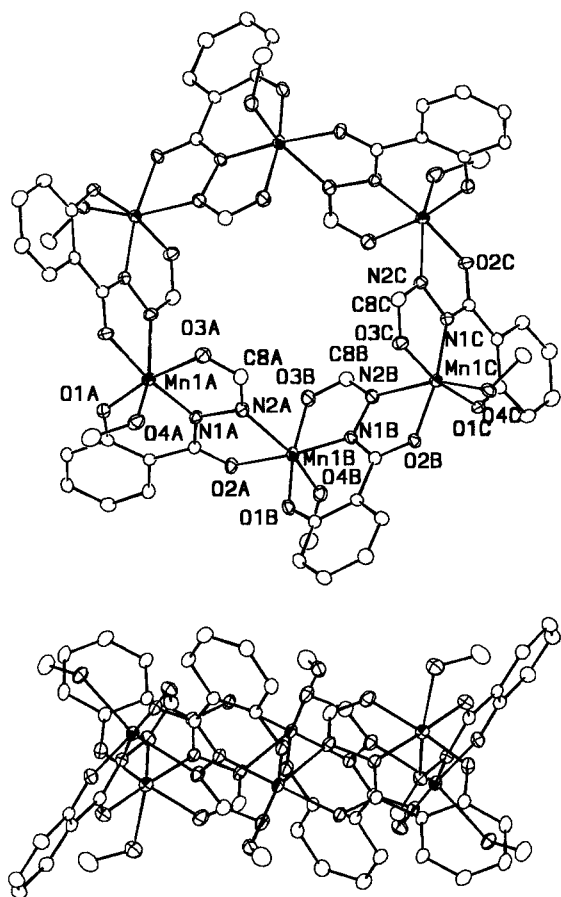


Figure 2. ORTEP drawing of complex **1**. (A) Top: Top view. Hydrogen atoms have been omitted for clarity. A, B, and C in the atom labels could be related to each other using a noncrystallographic S_6 symmetry operation. (B) Bottom: Side view.

deep.¹⁰ Even though several noncoordinating methanols are in the lattice and interact with the cluster using a hydrogen bond, none of them are located on the inside of the cavity.

Nine-membered metallacrowns always have metal centers in the propeller configuration, and all metal centers have the same chiralities.^{5a-c} However, the chiralities of the metal centers in complex **1** alternate between the Λ and Δ forms. The alternation of the chiralities expands the cyclic ring system of complex **1** to the 24-membered ring system. Each chiral metal center of the cluster has a solvent methanol coordinated. Three methanols coordinated at the metal centers with Λ configuration are in one face of the cluster, and the remaining three methanols coordinated at the other metal centers with Δ configurations are in the other face of the cluster. The two faces of the disc-shaped macrocyclic cluster have opposite chiralities to each other.

The crystal packing structure of complex **1** shows that the disc-shaped hexanuclear clusters are aligned approximately along the crystallographic a axis. The cavities of the clusters in the crystal structure are also aligned, and one-dimensional channels are formed. One of these channels is shown in Figure 3.

(10) The entrance diameter of the cavity was calculated using a CPK model. The three C8 atoms that are related by the noncrystallographic C_3 symmetry operation formed the entrance of the cavity. The largest diameter formed by the manganese atoms in the center of the cavity was calculated similarly using the CPK model. The depth of the cavity was calculated using the interplane distance between the two planes where each plane was formed by the noncrystallographic C_3 symmetry-related three C8 atoms.

Table 2. Bond Lengths (Å) and Angles (deg) for **1**

Mn1A—O1A	1.852 ^a	Mn1A—O2C	1.967
Mn1A—O3A	1.945	Mn1A—O4A	2.234
Mn1A—N1A	1.930	Mn1A—N2C	2.246
Mn1A—Mn1C ^b	8.031	C8A—C8C ^c	5.025
O1A—Mn1A—O2C	94.6	O1A—Mn1A—O3A	169.9
O1A—Mn1A—O4A	92.2	O1A—Mn1A—N1A	90.5
O1A—Mn1A—N2C	96.7	O3A—Mn1A—O2C	95.0
O2C—Mn1A—O4A	83.5	N1A—Mn1A—O2C	172.7
O2C—Mn1A—N2C	74.7	O3A—Mn1A—O4A	86.0
N1A—Mn1A—O3A	80.3	O3A—Mn1A—N2C	88.7
N1A—Mn1A—O4A	101.5	O4A—Mn1A—N2C	156.9
N1A—Mn1A—N2C	99.6		

^a This is an average value of the Mn1A—O1A, Mn1B—O1B, and Mn1C—O1C bond distances. Other average bond distances or angles are also calculated similarly. ^b This is an average value of the interatomic distances, Mn1A—Mn1C, and other two similar interatomic distances related by the noncrystallographic C_3 symmetry operation. ^c This is an average value of the interatomic distances, C8A—C8C, and other two similar interatomic distances related by the noncrystallographic C_3 symmetry operation.

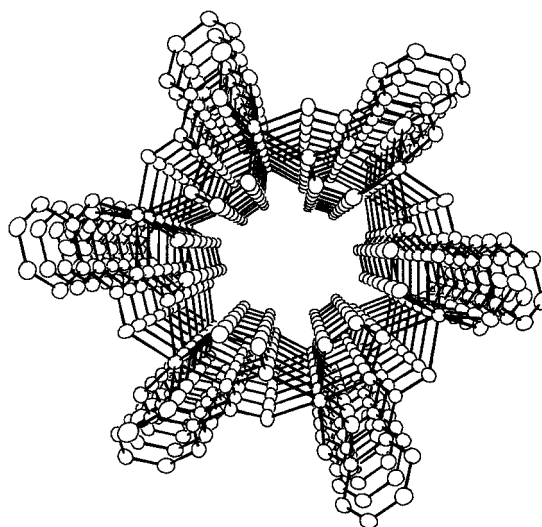


Figure 3. Cavities of the hexanuclear clusters aligning approximately along the crystallographic a axis in the crystal structure. The average intercluster distance is about 10 Å, which is the crystallographic repeat of the a axis. Noncoordinating methanols in the lattice are omitted.

The solution integrity of this cluster was addressed using solution mass spectrometry. The methanol solution of the cluster in a 3-nitrobenzyl alcohol matrix gave a peak at m/z 1393.5 in the FAB-MS. This peak corresponds to the cyclic hexanuclear cluster ion, $[\text{Mn}_6(\text{fshz})_6 + \text{H}]^+$. The solution integrity of the cluster was also confirmed using paramagnetically shifted ¹H NMR spectroscopy. The ¹H NMR spectrum of the complex in acetone-*d*₆ shows three peaks at -10.1, -21.6, and -34.9 ppm (Figure 4).¹¹ These peaks were tentatively assigned as the phenyl protons of the bridging ligands. Similar upfield peaks of the manganese metallacrowns were observed and assigned to the phenyl protons of the salicylhydroximate (shi^{3-}) ligand using deuterium exchange experiments.^{5d} The bridging mode of the shi^{3-} ligand in the metallacrown is very similar to that of the fshz^{3-} ligand in complex **1** (Figure 1). The diamagnetic region shows only one peak at 3.20 ppm. This peak was assigned to the protons of water molecules.¹² No peaks related to methanol could be observed even though the

(11) The spectrum does not change for at least 6 months.

(12) The peak shifts to 3.60 ppm at -50 °C. The peak intensity grows when a small amount of water is added to the solution.

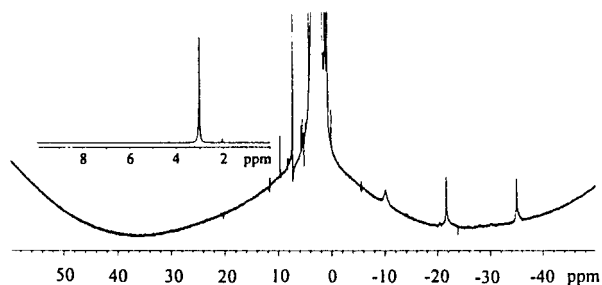


Figure 4. ^1H NMR spectrum of complex **1** in acetone- d_6 . Inset: Diamagnetic region of the spectrum.

crystal structure showed six coordinated methanol molecules and several structural methanol molecules. The elemental analysis result also agrees only with the cluster of six water molecules instead of methanol molecules. Probably the atmospheric water molecules exchanged the coordinate methanol molecules. To explore the solution stability of complex **1** at THF solution, the concentration-dependent absorbance was measured at 369 nm. The absorbance increases linearly with the concentration at the window between 2.0 and 62 μM .¹³ The result indicates that complex **1** is stable at least at the concentration ranges.

(13) A figure that shows the concentration-dependent absorbance of complex **1** at 369 nm is in the Supporting Information.

This new type of hexanuclear manganese cluster has a vacant cavity in the center of the cluster. In addition, the cluster keeps its structural integrity in solution. The vacant cavity and the formation of the one-dimensional channels by the alignment of the clusters suggest that this cluster might be a new type of inorganic host molecule. Due to the opposite chiralities of the two faces, the disc-shaped macrocyclic cluster might have interesting chiral recognition properties. Currently, we are expanding the system to other metal ions and studying the recognition chemistry of the hexanuclear cluster.

Acknowledgment. We thank the Korean Institute of Basic Science for elemental analyses and mass spectra and the National Institute of Technology and Quality for the use of an X-ray diffractometer. This work was supported by the KOSEF (Grant No. 941-0300-032-2) and the Basic Research Institute Program, Ministry of Education (Grant No. BSRI-97-3443), Republic of Korea.

Supporting Information Available: Tables giving the structure determination summary, atomic coordinates and temperature factors, bond lengths and bond angles, anisotropic thermal parameters, and atomic coordinates for hydrogen atoms, an ORTEP drawing with complete atomic numbering for complex **1**, and a figure showing the concentration dependent absorbance of complex **1** (14 pages). Ordering information is given on any current masthead page.

IC971538H